Integrated Ferroelectrics, 84: 165–174, 2006

ISSN 1058-4587 print / 1607-8489 online
DOI: 10.1080/10584580601085719

Taylor & Francis
Taylor & Francis Group

Preparation of $Pb(Zr_{0.35}Ti_{0.65})O_3$ Films on Conducting Oxide Ga-Doped ZnO Films for Transparent Ferroelectric Thin-Film Transistors

Kwang Bae Lee,[1] Kyung Haeng Lee,[1] and Byeung Kwon Ju[2,*]

[1]Department of Computer & Electronic Physics, Sangji University,
Wonju, Gangwon-do 220-702, Korea
[2]Department of Electrical Engineering, Korea University,
Sungbook-goo, Seoul 136-701, Korea

ABSTRACT

We have investigated the feasibility of the deposition of ferroelectric PZT films on transparent conducting Ga-doped ZnO (GZO) films, for transparent ferroelectric thin-film transistors. Low resistive and high c-axis oriented GZO films are prepared at the substrate temperature of 250°C using the dc magnetron sputtering method. PZT films are deposited at low substrate temperature and subsequently crystallized by means of the rapid annealing process in a high vacuum to minimize the reaction of PZT with GZO films. Various vacuum-annealing conditions are investigated to get high-quality PZT films, which show single perovskite phase with a random orientation. The optimized PZT/GZO capacitors have somewhat unsaturated P-E hysteresis loops with the values of remanent polarization and coercive field of about 4.5 $\mu C/cm^2$ and 145 kV/cm, respectively.

Keywords: Ferroelectric PZT films; transparent conducting Ga-doped ZnO (GZO); vacuum-annealing process; transparent TFTs

1. INTRODUCTION

The recent development of transparent thin-film transistors (TTFTs) represents a major advance in the emerging field of transparent electronics [1, 2]. TTFTs could find many applications in light-emitting displays, smart windows, solar cells, security or military systems, and even toys. Among the extensive

Received May 31, 2006.
*Corresponding author. E-mail: bkju@korea.ac.kr

approaches for TTFTs development, the gate insulator [3, 4], as well as the transparent conducting oxides [5–7] and the transparent semiconductor films [8, 9], in TTFTs has been the one of the important subjects being compatible with those of the next generation complementary metal-oxide-semiconductor technology. Especially, TFTs with a ferroelectric (FTFT) insulator have been the subject of numerous studies [10, 11] because of their memory function and non-destructive readout properties. While M. W. J. Prins et al. [12] reported a bottom-gated FTFT with a ferroelectric $Pb(Zr,Ti)O_3$ (PZT) on a $SrRuO_3$-conducting-oxide gate having tens-percents optical absorption, fully transparent FTFTs have not been accomplished yet.

In this study, the preparation conditions of ferroelectric PZT films were optimized for use with the bottom electrode of transparent conducting oxides (TCO) for the feasibility of fully transparent FTFTs. Especially, Ga-doped ZnO (GZO) films [7] were chosen as the bottom TCO electrodes for preparing ferroelectric PZT films. GZO films have been given attention to promise alternatives of Sn-doped In_2O_3 (ITO) [5], with advantages of low cost, resource availability, and nontoxicity. Moreover, because of GZO films with the high crystalline nature similar to c-axis oriented ZnO films, contrasted with amorphous-like ITO films, the GZO bottom electrodes were expected to be helpful to the crystallization process of PZT films.

2. EXPERIMENTAL

The deposition of GZO films on borosilicate glass substrates (Corning 7059) was carried out by the dc sputtering method, using self-made GZO targets with three Ga_2O_3 contents ($x = 4.0$, 5.3, 7.0 wt% in (1-x)ZnO-xGa_2O_3) of 2-inch-diameter. After the sputtering chamber was evacuated below 5×10^{-6} Torr, highly purified Ar and O_2 with the partial pressure of 7×10^{-4} Torr and 2×10^{-4} Torr, respectively, were fixed during deposition as the process gas inleted through mass flow controller. The dc power of 100 W was also fixed during deposition, in which the 200-nm-thickness GZO films were controlled by the deposition time.

The deposition of PZT films were carried out by the conventional rf sputtering method, using self-made PZT targets of 2-inch-diameter with the compositions of $Pb_{1.3}(Zr_{0.35}Ti_{0.65})O_3$. The GZO-deposited glass substrates (GZO/glass), as well as commercial Pt/Ti/SiO_2/Si wafers (Inostek Co.), were used for the deposition of PZT films, in which the former was used preliminarily to get the optimized conditions of sputter-deposition for high-quality PZT films. The partial pressures of 8×10^{-4} Torr and 5×10^{-4} Torr for Ar and O_2, respectively, as well as the rf power of 100 W, were fixed during deposition. The substrate temperature was fixed as 100°C during the deposition of PZT films and, after the deposition of PZT, the rapid annealing in a high vacuum of about 5×10^{-6} Torr (vacuum-annealing) were subsequently performed with the ramping rate of

50°C/min, as well as with various annealing durations at the annealing temperature around 550°C, in order to reduce the diffusion at the interface between PZT and GZO. The thickness of PZT films was about 250 nm and the temperature profiles were controlled by a programmable temperature controller.

The thickness of all specimens was evaluated using a reflectance spectrometer (ST-2000, K-Mac) and the electrical resistivity was measured by four-probe method using a source/meter unit (Keithley 2400). The structural properties were observed using X-ray diffraction (XRD) spectroscopy and the compositional analysis of GZO was determined using X-ray photoelectron spectroscopy (XPS). The P-E hysteresis loops of PZT capacitors were measured using a standardized ferroelectric tester (RT66A, Radiant Tech.).

3. RESULTS AND DISCUSSION

Figure 1 shows the XRD intensity of ZnO (200) peak at $2\theta = 34.8°$ for GZO films deposited at various substrate temperature (T_{sub}), in which the typical XRD patterns of GZO (x = 5.3 wt%) films were shown in the inset of Fig. 1. The XRD patterns of all GZO films were found to be the c-axis orientation. Especially, the XRD intensity of ZnO (200) peaks for a GZO (x = 5.3 wt%) film deposited at T_{sub} around 250°C was greatest, in which the grain size is about 36 nm, which was estimated from FWHM of the XRD peaks by the Scherrer method [13]. Such results shown in Fig. 1 were compatible with the electrical resistivity ρ of GZO films deposited at various T_{sub}, as shown in Fig. 2. The lowest resistivity of 3×10^{-4} Ωcm was obtained for GZO films (x = 5.3 wt%)

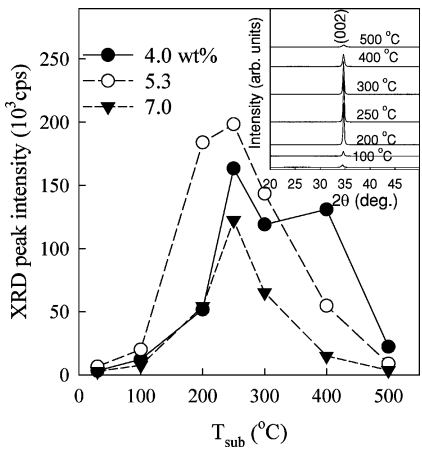

Figure 1. XRD intensity of ZnO (200) peak at $2\theta = 34.8°$ for GZO films deposited at various substrate temperature (T_{sub}). The inset shows the XRD patterns of GZO (x = 5.3 wt%) films.

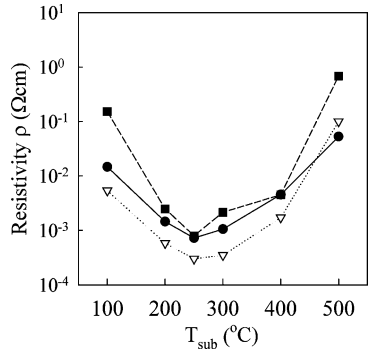

Figure 2. Plot of Resistivity ρ vs. T_{sub} for GZO films with various Ga_2O_3 contents.

deposited at T_{sub} of 250°C, which was nearly the same as the typical resistivity of the commercial ITO specimens [5]. These GZO films showed transparent with the optical transmittance greater than 80% in the visible region. Such high quality GZO films were thought to be due to the optimum oxygen contents in GZO, which were determined by the compositional analysis of XPS spectra of Zn $2p_{3/2}$, O 1s and Ga $2p_{3/2}$ core levels, as shown in Fig. 3. The ratio of O to Zn, O/Zn, was found to be about 1.0 for an optimized GZO specimen ($x = 5.3$ wt%, $T_{sub} = 250$°C), while the values of O/Zn for the other specimens were ranged from 1.10 to 1.20.

On the optimized GZO films as bottom electrodes, the deposition of PZT films was tried to begin by means of the conventional metal organic deposition (MOD) method, which was reported elsewhere [14]. Figure 4 shows the XRD patterns of MOD-PZT films deposited on GZO/glass substrates with the final

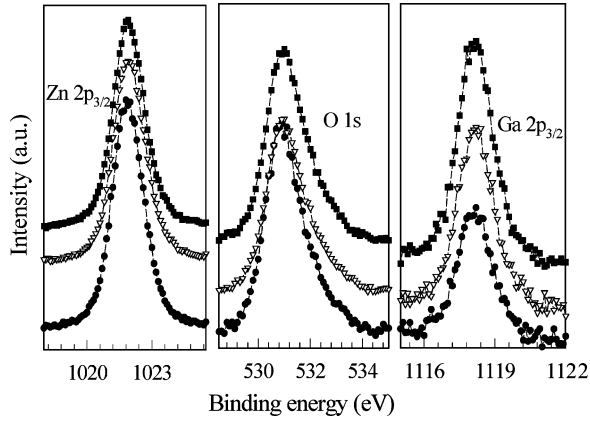

Figure 3. XPS spectra of Zn $2p_{3/2}$, O 1s and Ga $2p_{3/2}$ core levels for GZO films deposited at 250°C.

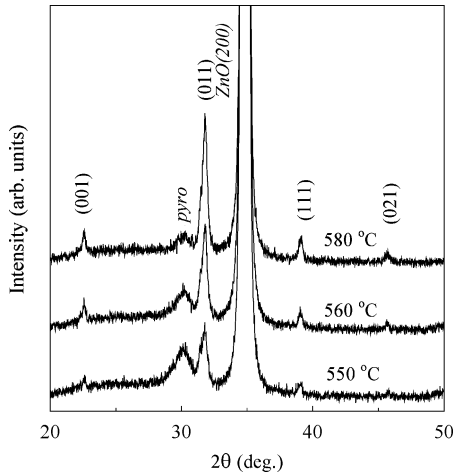

Figure 4. XRD patterns of MOD-PZT films annealed at various temperatures.

annealing temperatures greater than 550°C for 10 min. The pyrochlore phase, as well as perovskite PZT peaks, was found for all MOD-PZT films, as shown in Fig. 4. The single perovskite phase with no pyrochlore phase could not be obtained even for the annealing temperatures greater than 600°C. Moreover, as the annealing temperature above 400°C in oxygen ambience, the resistivity of GZO films increased seriously greater than by five orders and finally conducting GZO electrodes failed as insulators. Such serious changes in resistivity of the GZO film were found to be due to the changes of chemical binding states of Ga in ZnO, as shown in Fig. 5, which implied the modification of Ga additives in ZnO instead of the appropriate doping of Ga in ZnO. From the results in Fig. 5, as well as in Fig. 4, the MOD method could not be available and, hence, the rf magnetron sputtering method was adopted for the deposition of PZT films on GZO bottom

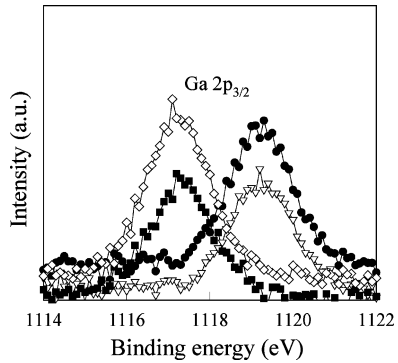

Figure 5. XPS spectra of Ga $2p_{3/2}$ core level for GZO films annealed at various temperatures in O_2 ambience.

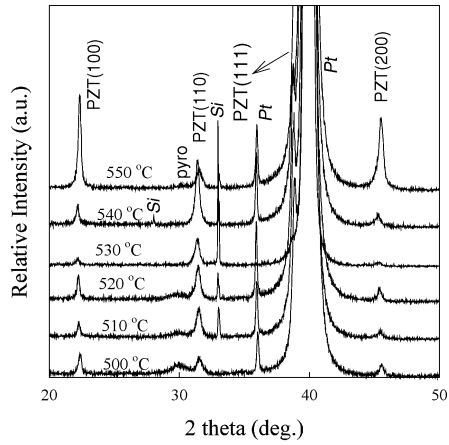

Figure 6. XRD patterns of PZT films deposited on $Pt/Ti/SiO_2/Si$ wafers for various vacuum-annealing temperatures.

electrodes. In order to maintain the properties of GZO electrodes during the deposition of PZT films, the *in-situ* vacuum-annealing process was carried out, which was mentioned above. Figure 6 shows the XRD patterns of PZT films deposited on $Pt/Ti/SiO_2/Si$ wafers vacuum-annealed for 2 min at various temperatures ranged from 500°C to 550°C. As shown in Fig. 6, PZT films with single perovskite phase could be obtained even for the vacuum-annealing at 530°C for 2 min. The ferroelectricity of these PZT films were confirmed using P-E hysteresis loops, as shown in Fig. 7. For PZT film capacitors with

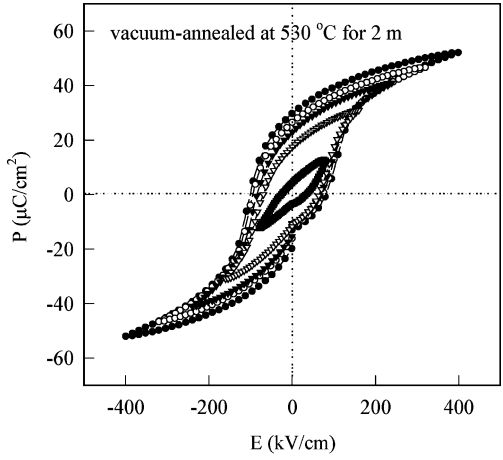

Figure 7. P-E hysteresis loops of a $PZT/Pt/Ti/SiO_2/Si$ capacitor vacuum-annealed at 530°C for 2 min.

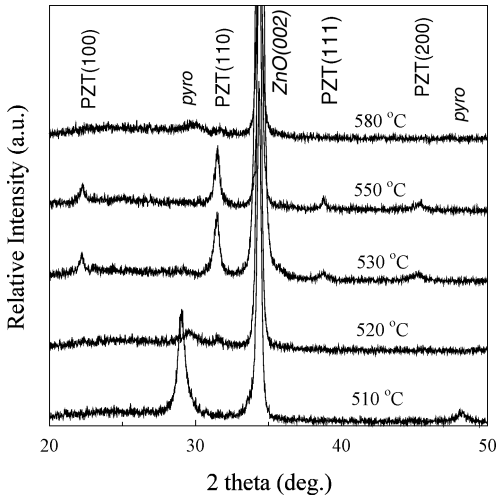

Figure 8. XRD patterns of PZT thin-films deposited on GZO films for various vacuum-annealed temperatures.

sputtered-Pt top electrodes of 3×10^{-4}-cm-diameter, the values of remanent polarization and coercive field at a field of 200 kV/cm were 15 μC/cm^2 and 80 kV/cm, respectively. PZT films deposited on GZO films were prepared referring to the process conditions obtained in Figs. 6 and 7.

Figure 8 shows the XRD patterns of PZT films deposited on GZO films vacuum-annealed for 2 min at various temperatures ranged from 510°C to 580°C. It could be found that for the vacuum-annealing temperatures ranged from 530°C to 550°C for 2 min, PZT films with single perovskite phase of random orientation were obtained, as shown in Fig. 8. Especially, for the vacuum-annealing temperature of 580°C, no XRD peak corresponding to PZT phases, except a ZnO (002) peak, could be appeared, which was compared with the XRD results in Fig. 4. Such absence of PZT peaks was assumed that during the vacuum-annealing process at temperatures greater than 580°C, the PZT layer would diffuse easily to the surface of GZO films and so failed the crystallization of PZT. This specimen was easily seen to be blurred, while the surface of PZT/GZO specimens vacuum-annealed at temperatures ranged from 530°C to 550°C was smooth and glossy. To get high-quality PZT films deposited on GZO films, the other process conditions for the vacuum-annealing, such as the deposition time, the ramping rate and the annealing duration, were investigated using the XRD measurements. While the XRD patterns of PZT/GZO specimens for such process conditions, however, were nearly the same in shape, as typically shown in Fig. 9, the surface of PZT/GZO specimens was somewhat distinguishable by using an optical microscope. The XRD patterns for various annealing durations ranged from 2 min to 30 min at 550°C showed nearly the same in shape, except for an short annealing duration of 1 min, but the

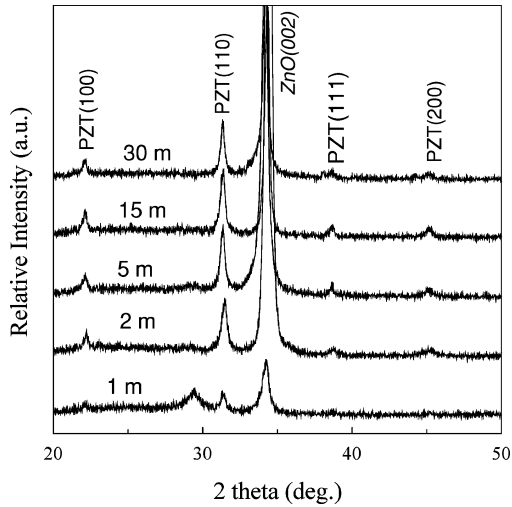

Figure 9. XRD patterns of PZT films deposited on GZO films for various annealing durations at 550°C.

longer annealing duration, the more microcracks could be observed. Hence, the vacuum-annealing temperature of 550°C and the annealing duration of 2 min, as well as the ramping rate of 50°C/min, for the preparation of high-quality PZT films were determined as optimum process conditions. Pt-top electrodes of 3×10^{-4}-cm-diameter were deposited on optimized PZT films by the dc sputtering method. The P-E hysteresis loops of these PZT film capacitors were shown in Fig. 10, which were found to be unsaturated in shape. Such unsaturated

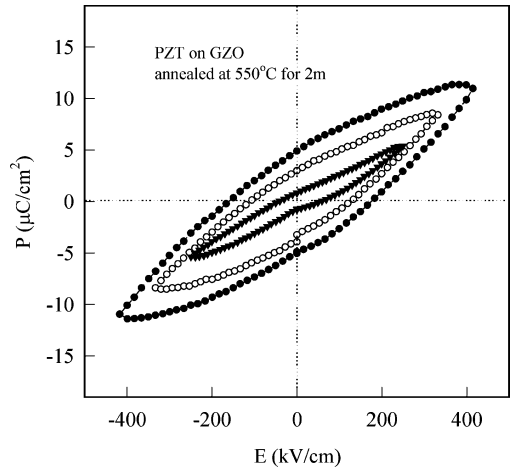

Figure 10. P-E hysteresis loops of a PZT/GZO capacitor vacuum-annealed at 550°C for 2 min.

P-E hysteresis loops were believed to be due to the diffusion around the interface between PZT and GZO even for the optimized PZT/GZO specimens, in which the values of remanent polarization and coercive field at a field of 200 kV/cm were estimated to be about 4.5 $\mu C/cm^2$ and 145 kV/cm, respectively. Further studies about the low temperature fabrication of transparent oxide semiconductors on optimized ferroelectric PZT films are being under investigated for the feasibility of transparent FTFTs.

4. CONCLUSION

The feasibility of the deposition of ferroelectric PZT films on transparent conducting GZO films has been investigated for the transparent FTFTs. Low resistive and high c-axis oriented GZO films were obtained by means of the dc magnetron sputtering method using GZO targets with a Ga_2O_3 content of 5.3 wt% at the substrate temperature of 250°C. The PZT films were deposited at low substrate temperature and were subsequently crystallized using the rapid annealing process in a high vacuum, in order to minimize the reaction of PZT with GZO films. Various vacuum-annealing conditions were investigated to get high-quality ferroelectric PZT films, in which the optimized PZT films could be prepared in the process conditions of the ramping rate of 50°C/min, the annealing temperature of 550°C and the duration of 2 min. The optimized PZT films deposited on GZO films showed single perovskite phase with random orientation, but had somewhat unsaturated P-E hysteresis loops with the values of remanent polarization and coercive field of about 4.5 $\mu C/cm^2$ and 145 kV/cm, respectively. Such possibilities of the deposition of ferroelectric PZT films on transparent conducting oxides should give expectations in the successive fabrications of fully transparent FTFTs.

REFERENCES

1. K. Nomura, H. Ohta, K. Ueda, T. Kamiya, M. Hirano, and H. Hosono, *Science* **300**, 1269 (2003).
2. R. L. Hoffman, B. J. Norris, and J. F. Wager, *Appl. Phys. Lett.* **82**, 733 (2003).
3. D. H. Kuo, C. H. Chien, and C. H. Huang, *Thin Solid Films* **420-421**, 47 (2002).
4. G. D. Wilk and R. M. Wallace, *Appl. Phys. Lett.* **74**, 2854 (1999).
5. Y. Shigesato and D. C. Paine, *Appl. Phys. Lett.* **62**, 1268 (1993).
6. H. Hara, T. Hanada, T. Shiro, and T. Yatabe, *J. Vac. Sci. Technol.* A **22**, 1726 (2004).
7. P. K. Song, M. Watanabe, M. Kon, A. Mitsui, and Y. Shigesato, *Thin Solid Films* **411**, 82 (2002).

8. K. Nomura, H. Ohta, A. Takagi, T. Kamlya, M. Hirano, and H. Hosono, *Nature* **432**, 488 (2004).
9. H. Q. Chiang, J. F. Wager, R. L. Hoffman, J. Jeong, and D. A. Keszler, *Appl. Phys. Lett.* **86**, 013503 (2005).
10. C. H. Seager, D. Mclntyre, B. A. Tuttle, and J. Evans, *Integrated Ferroelectrics* **6**, 47 (1995).
11. Y. Watanabe, *Appl. Phys. Lett.* **66**, 1770 (1995).
12. M. W. J. Prins, K.-O. Grosse-Holz, G. Müller, J. F. M. Cillessen, J. B. Giesberg, R. P. Weening, and R. W. Wolf, *Appl. Phys. Lett.* **68**, 3650 (1996).
13. H. P. Klug and L. E. Alexander, In *X-ray Diffraction procedures for Polycrystalline and Amorphous Material* 2nd ed., Wiley, New York, 1974, Chapter 9.
14. K. B. Lee and K. H. Lee, *Integrated Ferroelectrics* **64**, 305 (2004).